

# Ultrafast and low overhead training symbol based channel estimation in coherent $M$ -QAM single-carrier transmission systems

Mohamed Morsy-Osman,<sup>1,2,\*</sup> Mathieu Chagnon,<sup>1</sup> Qunbi Zhuge,<sup>1</sup> Xian Xu,<sup>1</sup> Mohammad E. Mousa-Pasandi,<sup>1</sup> Ziad A. El-Sahn,<sup>2</sup> and David V. Plant<sup>1</sup>

<sup>1</sup>Department of Electrical and Computer Engineering, McGill University, Montreal, Quebec H3A 2A7, Canada

<sup>2</sup>Department of Electrical Engineering, Alexandria University, Alexandria 21544, Egypt

\*mohamed.osman2@mail.mcgill.ca

**Abstract:** We propose a training symbol based channel estimation (TS-EST) algorithm that estimates the  $2 \times 2$  Jones channel matrix. The estimated matrix entries are then used as the initial center taps of the  $2 \times 2$  butterfly equalizer. Employing very few training symbols for TS-EST, ultrafast polarization tracking is achieved and tap update can be initially pursued using the decision-directed least mean squares (DD-LMS) algorithm to mitigate residual intersymbol interference (ISI). We experimentally verify the proposed TS-EST algorithm for 112 Gbps PDM-QPSK and 224 Gbps PDM-16QAM systems using 10 and 40 training symbols for TS-EST, respectively. Steady-state and transient bit error rates (BERs) achieved using the TS-EST algorithm are compared to those obtained using the constant modulus algorithm (CMA) and the training symbol least mean squares (TS-LMS) algorithm and results show that the proposed TS-EST algorithm provides the same steady-state BER with a superior convergence speed. Also, the tolerance of the proposed TS-EST algorithm to laser phase noise and fiber nonlinearity is experimentally verified. Finally, we show by simulation that the superior tracking speed of the TS-EST algorithm allows not only for initial polarization tracking but also for tracking fast polarization transients if four training symbols are periodically sent during steady-state operation with an overhead as low as 0.57%.

©2012 Optical Society of America

OCIS codes: (060.1660) Coherent communications; (060.2330) Fiber optics communications.

---

## References and links

1. K. Roberts, D. Beckett, D. Boertjes, J. Berthold, and C. Laperle, "100G and beyond with digital coherent signal processing," *IEEE Commun. Mag.* **48**(7), 62–69 (2010).
2. P. J. Winzer, "Beyond 100G Ethernet," *IEEE Commun. Mag.* **48**(7), 26–30 (2010).
3. X. Liu, S. Chandrasekhar, X. Chen, P. J. Winzer, Y. Pan, T. F. Taunay, B. Zhu, M. Fishteyn, M. F. Yan, J. M. Fini, E. M. Monberg, and F. V. Dimarcello, "1.12-Tb/s 32-QAM-OFDM superchannel with 8.6-b/s/Hz intrachannel spectral efficiency and space-division multiplexed transmission with 60-b/s/Hz aggregate spectral efficiency," *Opt. Express* **19**(26), B958–B964 (2011).
4. S. Chandrasekhar and X. Liu, "Experimental investigation on the performance of closely spaced multi-carrier PDM-QPSK with digital coherent detection," *Opt. Express* **17**(24), 21350–21361 (2009).
5. S. J. Savory, "Digital coherent optical receivers: algorithms and subsystems," *IEEE J. Sel. Top. Quantum Electron.* **16**(5), 1164–1179 (2010).
6. E. Ip and J. M. Kahn, "Fiber impairment compensation using coherent detection and digital signal processing," *J. Lightwave Technol.* **28**(4), 502–519 (2010).
7. E. Ip, A. P. Lau, D. J. Barros, and J. M. Kahn, "Coherent detection in optical fiber systems," *Opt. Express* **16**(2), 753–791 (2008).
8. M. G. Taylor, "Coherent detection method using DSP for demodulation of signal and subsequent equalization of propagation impairments," *IEEE Photon. Technol. Lett.* **16**(2), 674–676 (2004).
9. E. Ip and J. M. Kahn, "Compensation of dispersion and nonlinear impairments using digital backpropagation," *J. Lightwave Technol.* **26**(20), 3416–3425 (2008).
10. G. Li, "Recent advances in coherent optical communication," *Adv. Opt. Photon.* **1**(2), 279–307 (2009).

11. S. J. Savory, "Digital filters for coherent optical receivers," *Opt. Express* **16**(2), 804–817 (2008).
  12. P. J. Winzer, A. H. Gnauck, C. R. Doerr, M. Magarini, and L. L. Buhl, "Spectrally efficient long-haul optical networking using 112-Gb/s polarization-multiplexed 16-QAM," *J. Lightwave Technol.* **28**(4), 547–556 (2010).
  13. L. Liu, Z. Tao, W. Yan, S. Oda, T. Hoshida, and J. C. Rasmussen, "Initial tap setup of constant modulus algorithm for polarization de-multiplexing in optical coherent receivers," in *Optical Fiber Communication Conference*, OSA Technical Digest (Optical Society of America, 2009), paper OMT2.
  14. G. Agrawal, *Lightwave Technology: Telecommunication Systems* (Wiley & Sons, 2005), Chap. 3.
  15. M. Morsy-Osman, M. Chagnon, Q. Zhuge, X. Xu, M. E. Mousa-Pasandi, Z. A. El-Sahn, and D. V. Plant, "Training symbol based channel estimation for ultrafast polarization demultiplexing in coherent single-carrier transmission systems with M-QAM constellations," in *Proceedings of European Conference and Exhibition on Optical Communication 2012*, paper Mo.1A.4.
  16. M. G. Taylor, "Phase estimation methods for optical coherent detection using digital signal processing," *J. Lightwave Technol.* **27**(7), 901–914 (2009).
  17. P. Ciblat and M. Ghogho, "Blind NLLS carrier frequency-offset estimation for QAM, PSK, and PAM modulations: performance at low SNR," *IEEE Trans. Commun.* **54**(10), 1725–1730 (2006).
  18. W. Shieh and K. P. Ho, "Equalization-enhanced phase noise for coherent-detection systems using electronic digital signal processing," *Opt. Express* **16**(20), 15718–15727 (2008).
  19. Q. Zhuge, X. Xu, Z. A. El-Sahn, M. E. Mousa-Pasandi, M. Morsy-Osman, M. Chagnon, M. Qiu, and D. V. Plant, "Experimental investigation of the equalization-enhanced phase noise in long haul 56 Gbaud DP-QPSK systems," *Opt. Express* **20**(13), 13841–13846 (2012).
  20. I. Fatadin, D. Ives, and S. J. Savory, "Blind equalization and carrier phase recovery in a 16-QAM optical coherent system," *J. Lightwave Technol.* **27**(15), 3042–3049 (2009).
  21. L. Nelson, "Polarization effects in coherent systems," in *Optical Fiber Communication Conference*, OSA Technical Digest (Optical Society of America, 2012), paper OTu1A.4.
  22. L. Nelson, M. Birk, S. L. Woodward, and P. Magill, "Field measurements of polarization transients on a long-haul terrestrial link," in *Proceedings of IEEE Photonics Conference 2011*, paper ThT5.
- 

## 1. Introduction

Digital coherent detection combined with  $M$ -ary quadrature amplitude modulation ( $M$ -QAM) and optical superchannel multiplexing techniques are envisioned to meet the growing need for higher capacity in future optical transport systems [1–4]. Also, a DSP-based coherent transceiver has the additional power to post-compensate and/or pre-compensate linear and nonlinear fiber transmission impairments [5–11]. In addition, coherent detection of both in-phase (I) and quadrature (Q) signals on both field polarizations enables the use of polarization division multiplexing (PDM) as an efficient way to double spectral efficiency in optical transport systems [5,7]. Along the fiber, the signal suffers from linear impairments such as chromatic dispersion (CD), random polarization rotation and polarization mode dispersion (PMD) [5,6]. Using a polarization-diversity coherent receiver, CD is first compensated by a static frequency domain equalizer (FDE) [5,6]. Then, the two transmitted orthogonal polarizations are reconstructed by a  $2 \times 2$  butterfly equalizer that mitigates polarization crosstalk and inter-symbol interference (ISI) due to PMD, filtering effects, and residual CD [5,6]. Several algorithms have been used for adapting the taps of the butterfly equalizer. Data-aided schemes are widely used where training symbols (TS) are sent and used at the receiver for tap adaptation using the least mean squares (LMS) algorithm [6]. Such TS based schemes reduce throughput due to the relatively large TS overhead required and have synchronization issues to locate TS. Therefore, blind techniques that exploit special data properties are preferred. One example of blind schemes is the constant modulus algorithm (CMA) which is widely used for quadrature phase shift keying (QPSK) modulation [5,11]. Even for high order quadrature amplitude modulations (QAMs) having non constant modulus, e.g. 16QAM, CMA still achieves reasonable pre-convergence after which adaptation is switched to decision-directed LMS (DD-LMS) for steady-state operation [12]. However, CMA usually provides slower convergence compared to TS based approaches and also has a singularity problem where both output polarizations of the butterfly equalizer converge to one transmitted polarization [13]. In general, convergence speed of all adaptive algorithms depend on the state of polarization (SOP) of received light, tap initialization and the step size parameter used for adaptively updating the taps.

In this paper, we present a novel TS based channel estimation (TS-EST) algorithm that utilizes a very small TS overhead to estimate the  $2 \times 2$  Jones channel matrix in a non-adaptive way thus allowing for ultrafast polarization tracking. The proposed TS-EST algorithm is

based on the fact that modern fibers have very small PMD parameter ( $< 0.1$  ps/km<sup>1/2</sup>) [14], and hence the channel can be assumed flat in the frequency domain given that the residual ISI is small since CD is initially compensated. The estimated matrix entries are then used to set the initial center taps of a butterfly equalizer. As polarization crosstalk is mitigated, initial constellations are reasonably compact such that decision-directed (DD) steady-state adaptation can be started after as few as 40 training symbols for TS-EST, thus achieving ultrafast polarization demultiplexing. Our algorithm is experimentally verified on both 112 Gbps PDM-QPSK and 224 Gbps PDM-16QAM systems and compared with TS-LMS and CMA. Results reveal that the proposed TS-EST algorithm achieves the same steady-state BER with a superior convergence speed compared to CMA and TS-LMS algorithms. Extending our work in [15], the tolerance of the proposed TS-EST algorithm to laser phase noise and fiber nonlinearity is experimentally verified using DFB lasers and high launch power scenario. Finally, we show by simulation that the superior tracking speed of the TS-EST algorithm allows not only for initial polarization tracking but also for tracking very fast polarization transients during steady-state operation. This can be done by sending four training symbols periodically with an overhead as low as 0.57% and exploiting them to periodically estimate the channel matrix and re-update the center taps of the butterfly equalizer before resuming adaptation using the DD-LMS algorithm.

## 2. Principle of proposed algorithm

Assuming CD is first compensated by a static FDE, PMD and polarization dependent loss (PDL) are negligible, and fiber nonlinearity is relatively small, a fiber channel can be considered flat in the frequency domain and modeled as a unitary  $2 \times 2$  Jones matrix  $\mathbf{R}$

$$\mathbf{R} = \begin{bmatrix} a & b \\ -b^* & a^* \end{bmatrix} \quad (1)$$

$$a = e^{j\delta} \cos \theta, \quad b = e^{j\varphi} \sin \theta \quad (2)$$

where  $2\theta$  and  $\varphi$  are the azimuth and elevation rotation angles, respectively, whereas  $2\delta$  is a differential phase between the two polarizations [5]. Assuming Nyquist pulses and using Eq. (1), the received signal  $\mathbf{S}_{rx}[n] = [s_{rx}^x[n] \quad s_{rx}^y[n]]^T$  can be expressed as

$$\mathbf{S}_{rx}[n] = e^{j\psi[n]} \mathbf{R} \mathbf{S}_{tx}[n] = e^{j\psi[n]} \begin{bmatrix} a s_{tx}^x[n] + b s_{tx}^y[n] \\ -b^* s_{tx}^x[n] + a^* s_{tx}^y[n] \end{bmatrix} \quad (3)$$

where  $\mathbf{S}_{tx}[n] = [s_{tx}^x[n] \quad s_{tx}^y[n]]^T$  is the transmitted signal and  $\psi[n]$  is the instantaneous phase of the  $n^{\text{th}}$  symbol originating from laser phase noise  $\psi_{pn}[n]$  and frequency offset  $\Delta f$  as follows

$$\psi[n] = 2\pi\Delta f T + \psi_{pn}[n] \quad (4)$$

The principle of the proposed algorithm is to send short special training symbols on X and Y polarizations and use the received data to estimate  $\mathbf{R}$  regardless of laser phase noise and frequency offset. Basically, we send  $N$  training symbols  $\mathbf{T}_{tx}[k]$ , where  $k \in [0, N-1]$ , designed such that:  $\mathbf{T}_{tx}[k] = c e^{j\xi} [1 \quad 1]^T$  and  $\mathbf{T}_{tx}[k+1] = c e^{j\xi} [1 \quad -1]^T$ , where  $\xi \in \{\pm\pi/4, \pm3\pi/4\}$  and  $c$  is a normalization constant that is chosen depending on the modulation format such that we send one of the four constellation corner symbols on the X and Y polarizations for the training period where the phase shift between every two successive polarization multiplexed training symbols alternates between 0 and  $\pi$ . Using Eq. (3), we can write the received training symbols as

$$\mathbf{T}_{rx}[k] = ce^{j(\xi+\psi[k])} \begin{bmatrix} a+b \\ -b^*+a^* \end{bmatrix}, \quad \mathbf{T}_{rx}[k+1] = ce^{j(\xi+\psi[k+1])} \begin{bmatrix} a-b \\ -b^*-a^* \end{bmatrix} \quad (5)$$

Knowing that  $\psi[k] \approx \psi[k+1]$  since laser phase noise is a slower process compared to the baud rate [16] and that  $\mathbf{R}$  is unitary, if we normalize the received training symbols in Eq. (5) to unit envelope, we can get

$$|a| \approx \sqrt{0.5 \left( 1 + \frac{1}{N} \operatorname{Re} \left\{ \sum_{i=0}^{N/2-1} \begin{pmatrix} T_{rx}^x[2i]T_{rx}^{x*}[2i+1] - \dots \\ T_{rx}^y[2i]T_{rx}^{y*}[2i+1] \end{pmatrix} \right\} \right)} \quad (6)$$

$$|b| \approx \sqrt{1 - |a|^2} \quad (7)$$

$$\arg\{a\} + \arg\{b\} = \arg \left\{ - \sum_{i=0}^{N/2-1} \begin{pmatrix} T_{rx}^x[2i]T_{rx}^{y*}[2i+1] + \dots \\ T_{rx}^{y*}[2i]T_{rx}^y[2i+1] \end{pmatrix} \right\} \quad (8)$$

Then, if the inverse of the matrix  $\mathbf{R}_1$  given by

$$\mathbf{R}_1 = \begin{bmatrix} |a| & |b|e^{j(\arg\{a\}+\arg\{b\})} \\ -|b|e^{-j(\arg\{a\}+\arg\{b\})} & |a| \end{bmatrix} \quad (9)$$

is left multiplied by  $\mathbf{R}$ , this yields zeros on the off-diagonal elements which achieves perfect polarization demultiplexing. Theoretically, the lowest number of training symbols required to perform TS-EST according to above equations is 2. However, in a noisy environment and low OSNR levels after long transmission distances, the  $\sum$  operation in Eqs. (6) and (8) is needed to average the estimates over  $N$  training symbols where  $N > 2$ . Furthermore, the differential phase between the two polarizations  $2\delta$  can be also estimated if we apply the inverse of  $\mathbf{R}_1$  back to the received training symbols and estimate the common phase difference between the demultiplexed training symbols.

After polarization demultiplexing is achieved, we can use the above estimates to set the initial center taps of a standard butterfly 2x2 equalizer whose remaining job is to mitigate any residual ISI. However, since polarization cross-talk is already mitigated, the constellations obtained by merely applying the inverse channel matrix estimated in Eqs. (6)-(8) are reasonably good to the extent that decision-directed (DD) error calculation can be pursued to update the taps of the butterfly filter using the DD-LMS algorithm after the short TS period. Since TS-EST is not an adaptive algorithm, the TS period used for estimation can be very short leading to very small TS overhead and ultrafast polarization tracking. As will be experimentally demonstrated hereafter, we used  $N$  as short as 10 and 40 for PDM-QPSK and PDM-16QAM, respectively.

### 3. Experimental setup and offline DSP

The proposed algorithm was verified experimentally for both 28 Gbaud PDM-QPSK and PDM-16QAM systems using the setup in Fig. 1(a). The in-phase (I) and quadrature (Q) signals were generated from either pulse pattern generators (PPGs) for PDM-QPSK or digital-to-analog converters (DACs) for PDM-16QAM. The I and Q signals were fed to a QAM transmitter to modulate either an external cavity laser (ECL) laser having a linewidth less than 100 kHz or a distributed feedback (DFB) laser with a 2.4 MHz linewidth depending on whether low or high phase noise scenario is considered. Single polarization power eye diagrams after the QAM transmitter are shown in the insets of Fig. 1(a) for both QPSK and 16QAM. Using a polarization beam splitter (PBS), an optical delay line (ODL) and a polarization beam combiner (PBC), PDM was emulated with a decorrelation delay of 324

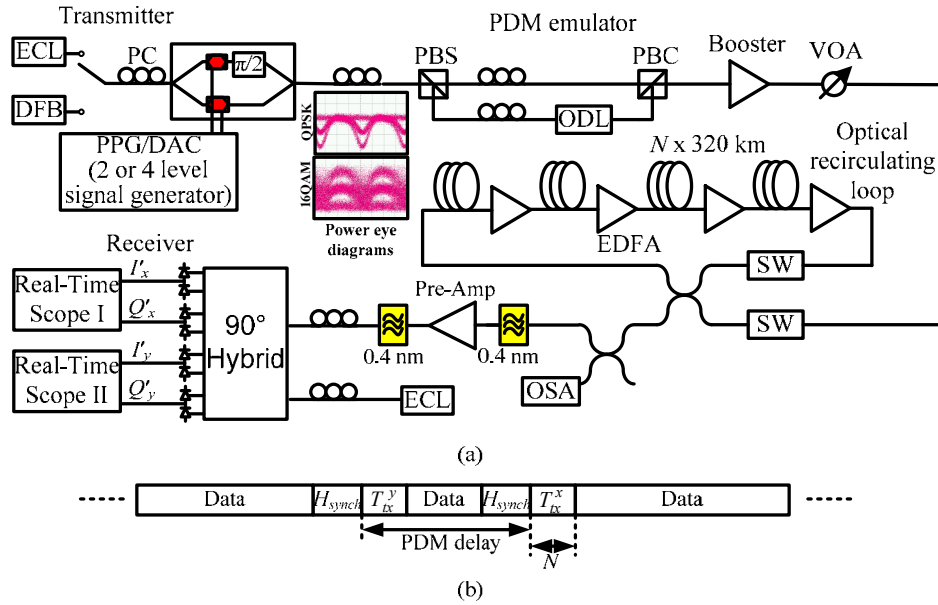


Fig. 1. (a) Experimental setup (PBS: Polarization Beam Splitter, PBC: Polarization Beam Combiner, VOA: Variable Optical Attenuator, SW: Optical Switch, ODL: Optical Delay Line, PC: Polarization Controller), (b) Training symbols and framing synchronization header.

symbols. The PDM signal was launched into an optical recirculating loop where each loop contains 4 spans of 80 km of SMF-28e<sup>+</sup> low loss fiber and an erbium-doped fiber amplifier (EDFA) with 5 dB noise figure. Then, the output signal from the loop is filtered by a 0.4 nm filter, pre-amplified and re-filtered by a 0.4 nm filter before coherent reception. Coherent reception is done using a 90° optical hybrid that mixes the signal with CW light from an ECL laser similar to the one used at the transmitter. After balanced detection, the four signals were sampled by two real-time scopes each running at 80 GSa/s for offline processing.

Since PDM was emulated in our experimental setup, we could not send different data on the two polarizations. Hence, our training symbols explained in the previous sections were inserted into the transmitted data by sending  $N$  training symbols  $T_{tx}^x[n]$  and  $T_{tx}^y[n]$  separated in time by the decorrelation delay used for PDM emulation, i.e. 324 symbols, as explained in Fig. 1(b). This will result in having  $T_{tx}^x[n]$  and  $T_{tx}^y[n]$  aligned in time at the two transmitted orthogonal polarizations after the PDM emulator.

Offline digital signal processing (DSP) at the receiver side starts by IQ imbalance compensation, resampling to 2 samples per symbol and CD compensation using a static FDE. Since the TS-EST algorithm is a data aided approach, frequency offset compensation has to be done before polarization demultiplexing. For that reason, the periodogram method [17] was chosen since it still works if there is polarization crosstalk prior to getting into the butterfly equalizer. Then, synchronization is performed to locate the  $N$  training symbols within the received data. Since training symbols added for polarization demultiplexing do not have good auto-correlation properties, cross-correlating the received symbols with the known TS would not produce a distinct peak to locate them. Hence, for synchronization purpose, 100 random symbols are sent in a header ( $H_{synch}$ ) prior to the TS used for polarization demultiplexing as shown in Fig. 1(b). At the receiver side, a peak is located by cross-correlating the received symbols with the known synchronization header from which the location of the TS that follows the header is automatically found. For polarization demultiplexing, we compare our proposed training symbol based channel estimation (TS-EST) with TS-LMS and CMA to achieve initial polarization tracking. After initial

convergence is achieved by either TS-EST or TS-LMS, we switch to DD-LMS for steady-state operation. In case of CMA, we keep using it for steady-state operation for PDM-QPSK, whereas we also switch to DD-LMS for PDM-16QAM depending on when CMA pre-converges to a reasonably compact constellation. We used step sizes of  $1 \times 10^{-3}$ ,  $1 \times 10^{-3}$  and  $4 \times 10^{-4}$  for TS-LMS, CMA and DD-LMS, respectively. For TS-EST, we used 10 and 40 training symbols for PDM-QPSK and PDM-16QAM, respectively to estimate the  $2 \times 2$  Jones matrix. Finally, phase noise was mitigated by a decision-directed first order phase locked loop (DD-PLL) with a loop coefficient of 0.02. The DD-PLL was either interleaved with the DD-LMS algorithms for steady-state operation or placed after the butterfly equalizer if CMA was used at steady-state in case of PDM-QPSK. Differential encoding / decoding was used to mitigate the angle ambiguity and cycle slips for all PDM-QPSK results. On the other hand, we used absolute encoding / decoding in case of PDM-16QAM to remove the penalty introduced by differential decoding. In order to resolve the angle ambiguity in case of absolute decoding, we used 100 pilot symbols at the beginning of our symbols and we did not encounter any cycle slips in all PDM-16QAM experimental data collected.

To verify how good the Jones matrix estimates provided by the proposed TS-EST algorithm are, we plot in Fig. 2(b) the constellations after 320 km for both PDM-QPSK and PDM-16QAM obtained by merely applying the estimated inverse Jones matrix using the proposed TS-EST scheme, *i.e.* before the butterfly equalizer and the PLL. This proves that polarization demultiplexing is indeed achieved using very low TS overhead. This allows the subsequent butterfly equalizer to operate in DD mode if initialized according to TS-EST. Figure 2(c) shows the final resulting constellations after the butterfly equalizer and the PLL. On the other hand, we always used 1500 training symbols for TS-LMS since it was the most needed to switch to DD-LMS in all collected data sets.

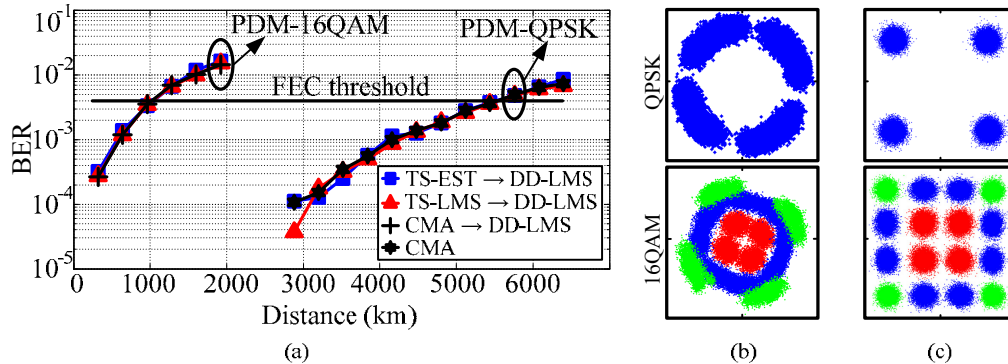


Fig. 2. (a) Steady-state BER versus distance for all algorithms for both PDM-QPSK and PDM-16QAM, (b) Constellations after 320 km transmission for both PDM-QPSK and PDM-16QAM obtained by merely applying the inverse Jones matrix obtained by TS-EST, (c) Constellations of the same case in (d) after the butterfly filter updated using DD-LMS and carrier recovery using DD-PLL.

## 4. Results and discussion

### 4.1 Low phase noise and low launch power scenario

In this subsection, we experimentally study the performance of our proposed TS-EST algorithm in a low phase noise and low launch power scenario. Throughout this subsection, ECLs were used as transmit and LO lasers and an optimum launch power of  $-2$  dBm was set. Steady-state and transient performance of the TS-EST scheme is compared to standard adaptive algorithms used for polarization demultiplexing.

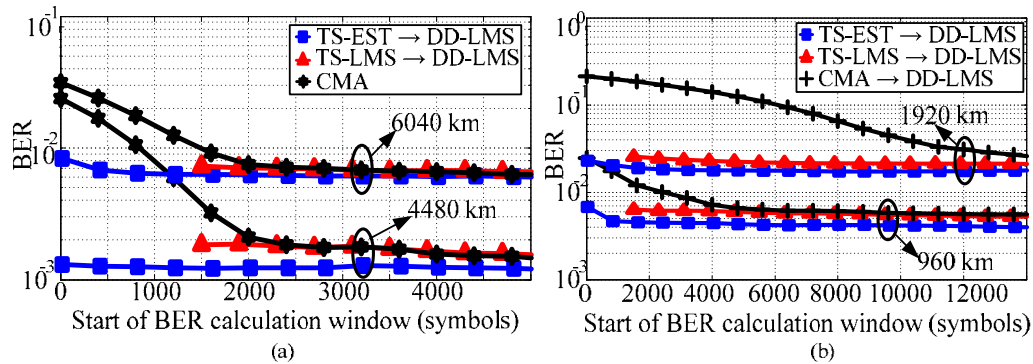


Fig. 3. Transient BER for all algorithms for (a) PDM-QPSK, (b) PDM-16QAM.

In Fig. 2(a), we first compare all the polarization demultiplexing algorithms in steady-state operation for both PDM-QPSK and PDM-16QAM. Steady-state bit-error-rates (BER) are calculated excluding the convergence period. All algorithms achieve similar steady-state BER allowing us to transmit 5400 and 1000 km below a FEC threshold of  $3.8 \times 10^{-3}$  for PDM-QPSK and PDM-16QAM, respectively.

Secondly, the speed of convergence of the algorithms is compared. A smaller window of 20000 symbols over which BER is calculated is swept starting right after the training period. In case of CMA, the window was swept from the first symbol as no training is needed. Figure 3(a) shows the results for PDM-QPSK at two different transmission distances of 4480 and 6080 km. Compared to TS-LMS, our proposed TS-EST scheme uses only 20 training symbols to achieve almost the same BER provided by TS-LMS using 1500 training symbols resulting in a huge reduction in TS length and very fast polarization tracking. Compared to around 2500 symbols needed by CMA, TS-EST achieves much faster convergence as well. It is also noteworthy that the speed of convergence achieved by our scheme does not depend on the SOP of the received light, whereas both TS-LMS and CMA might achieve a faster or slower convergence depending on the SOP, tap initialization and the step size parameter used for adaptation. Also, our scheme inherently does not suffer from any singularity problems and has the advantage that the transmitted X and Y polarizations are always recovered at the output X and Y polarizations, respectively. Finally, we compare all algorithms for PDM-16QAM after 960 and 1920 km. As seen in Fig. 3(b), TS-LMS needs 1500 symbols before switching to DD operation compared to around 3000 and 8500 symbols needed by CMA at both distances, respectively. On the other hand, since TS-EST needed only 40 training symbols before switching to steady-state DD operation, it is very difficult to visualize such a short convergence period in Fig. 3(b).

#### 4.2 High phase noise and high launch power scenario

In this subsection, we experimentally study the performance of our proposed TS-EST algorithm in a high phase noise and high launch power scenario. This aims at evaluating the tolerance of the TS-EST algorithm against large phase noise and high fiber nonlinearity to validate the assumptions upon which the channel model used in section (2) to propose the algorithm.

In Fig. 4(a), we first plot the steady-state BER versus distance of the TS-EST algorithm for PDM-QPSK in the high phase noise and high launch power scenarios. For the high laser phase noise scenario, a 2.4 MHz DFB laser was used as the transmit laser while keeping an ECL as the LO in order not to add an additional penalty from equalization enhanced phase noise (EPPN) [18,19]. For the high launch power case, 2dBm was launched into the recirculating loop to have high fiber nonlinearity. For comparison, we also plot the steady-



state BER for the case of having  $-2$  dBm launch power and two ECLs as transmit and LO lasers.

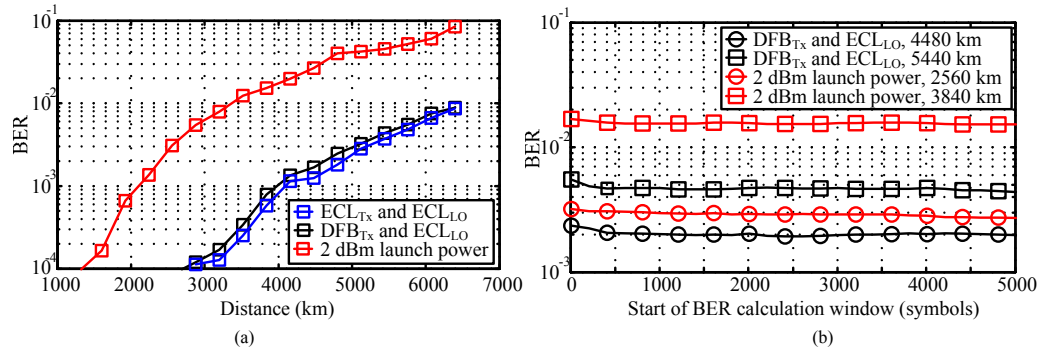


Fig. 4. BER for the TS-EST algorithm for PDM-QPSK in both high phase noise and high launch power scenarios for: (a) steady-state, (b) transient cases.

In all scenarios, TS-EST using 10 training symbols was used for polarization demultiplexing. We notice that the TS-EST algorithm works well in both scenarios. For the high phase noise scenario, the BERs achieved are so close to the ones obtained when using an ECL as the transmit laser because the loop coefficient of the DD-PLL was optimized to mitigate the larger phase noise. However, for the 2dBm launch power case, BERs are about an order of magnitude higher than the optimum launch power case because we did not use any nonlinearity mitigation scheme. However, this penalty does not originate from using the TS-EST algorithm for initializing the butterfly equalizer because the transient BER curves shown in Fig. 4(b) show that after 10 training symbols the initial BERs were very close to the steady-state BERs achieved after switching to DD-LMS steady-state operation for both 2560 and 3840 km transmission. Figure 4(b) also shows that TS-EST still provides very fast convergence with very small TS overhead for both high laser phase noise and high fiber nonlinearity scenarios.

#### 4.3 TS-EST algorithm for tracking fast SOP transients

In this subsection, we show by simulation that the superior tracking speed and low TS overhead (OH) required by the proposed TS-EST algorithm cannot only be used for initial polarization demultiplexing at startup but also for tracking fast SOP transients at steady-state operation.

Simulations were done in an optical back-to-back configuration for both 14 Gbaud and 28 Gbaud PDM-16QAM at an OSNR level 3 dB higher than the theoretical required OSNR to achieve a FEC threshold of  $3.8 \times 10^{-3}$ . To study the effect of SOP transients on the steady-state BER, we multiply the Jones vector of the transmitted symbols by the Jones matrix  $\mathbf{R}$  [20]

$$\mathbf{R} = \begin{bmatrix} \cos \omega t & \sin \omega t \\ -\sin \omega t & \cos \omega t \end{bmatrix} \quad (10)$$

where  $\omega$  is the angular frequency of the SOP changes. Multiplying by  $\mathbf{R}$  given in (10) simulates an endless polarization rotation at a constant rate. Transmit and LO laser linewidths were 100 kHz and a total of 448000 symbols were transmitted. Since the focus in this subsection is not on the initial convergence of all polarization demultiplexing algorithms, we only calculate the steady-state BER in all cases by excluding the first 40000 symbols to allow all algorithms to converge. Steady-state BER values will depend on how each algorithm used for steady-state operation is able to track the endless time-varying SOP introduced by  $\mathbf{R}$  in (10). For the TS-EST algorithm to be able to track dynamically varying SOP, we transmit 4



training symbols every 700 symbols as shown in Fig. 5(a) which corresponds to a very small overall overhead of 0.57%. For this overhead, the TS transmission rate is 20 MHz and 40 MHz at 14 and 28 Gbaud, respectively, which allows tracking very fast SOP transients as will be shown. It is noteworthy that no extra overhead is needed to perform synchronization to locate the TS within the received data since synchronization has already been achieved at startup and training symbols are sent periodically every 700 symbols at steady-state operation. After using TS-EST every 700 symbols using the 4 training symbols, we use the newly found Jones matrix estimates to update the center taps of the butterfly equalizer and continue operating using the DD-LMS operation until the next TS period.

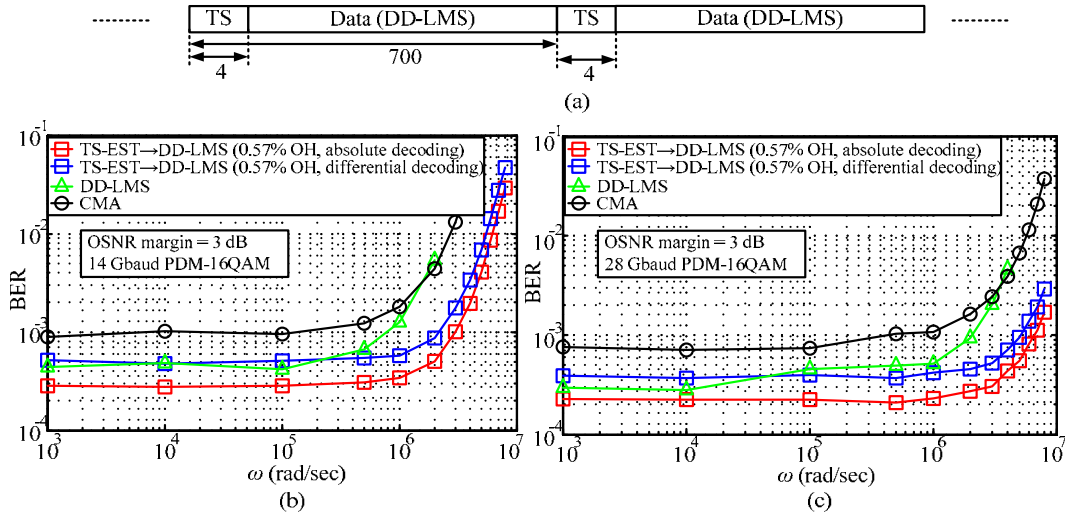


Fig. 5. (a) Periodic training symbols for SOP tracking, (b) Steady-state BER versus SOP angular frequency for different algorithms for 14 Gbaud PDM-16QAM, (c) Steady-state BER versus SOP angular frequency for different algorithms for 28 Gbaud PDM-16QAM.

In Figs. 5(b) and 5(c), we plot the steady-state BER versus the SOP angular frequency ( $\omega$ ) for both 14 Gbaud and 28 Gbaud PDM-16QAM, respectively. Although high speed SOP transients happen as rare events in a real system and will cause system outages [21,22], we use a fixed  $\omega$  for each point on Figs. 5(b) and 5(c) to simplify the simulation as well as characterize the tracking limits of all algorithms. We compare three polarization demultiplexing algorithms at steady-state: 1) TS-EST every 700 symbols and using DD-LMS for the data symbols within the TS period, 2) DD-LMS, and 3) CMA. For the case of TS-EST, as TS are sent periodically every 700 symbols to be used for channel estimation, those TS can be also used to resolve the angle ambiguity and cycle slip problem and hence, absolute decoding can be used instead of differential decoding. Thus, we also show both cases on Figs. 5(b) and 5(c). For DD-LMS, we use TS-LMS for the initial tracking before switching to DD-LMS for steady-state operation. In both 14 and 28 Gbaud cases, our TS-EST algorithm considerably improves the tracking performance of the DD-LMS algorithm at the expense of 0.57% overhead. We should also note that if DD-LMS is used, a real system has to go back to training mode and uses TS-LMS if the adaptive equalizer loses polarization tracking and the BER deteriorates because DD-LMS is not going to be able to re-track the fast varying channel. However, the TS overhead needed for TS-LMS to re-track the channel is much larger than the TS overhead needed for our TS-EST algorithm especially because no synchronization is further needed. Finally, it is clear that CMA provides a considerably worse performance if used at steady-state for 16QAM since it is a multi ring constellation.

## 5. Conclusion

Low overhead training symbol based estimation (TS-EST) of the Jones channel matrix is proposed. With fewer than 40 training symbols, tap adaptation of a butterfly equalizer can be started in DD mode. The proposed scheme is experimentally verified for 28 Gbaud PDM-QPSK and PDM-16QAM and found to achieve superior convergence speed compared to standard algorithms. Also, the proposed TS-EST algorithm is verified to be tolerable to large phase noise and high fiber nonlinearity scenarios. Finally, we also showed by simulation that the superior speed and simplicity of the TS-EST algorithm can also be beneficial for tracking fast polarization transients if four training symbols are periodically sent during steady-state operation with an overhead as low as 0.57%.